Journal of Power Sources 199 (2012) 37–45

Contents lists available at SciVerse ScienceDirect

Journal of Power Sources

journal homepage: www.elsevier.com/locate/jpowsour

Fabrication of anion-exchange composite membranes for alkaline direct methanol fuel cells

Chun-Chen Yang*, Sheng-Shin Chiu, Shih-Chen Kuo, Tzong-Horng Liou

Department of Chemical Engineering, Mingchi University of Technology, New Taipei City 24301, Taiwan, ROC

ARTICLE INFO

Article history:
Received 2 September 2011
Received in revised form 3 October 2011
Accepted 6 October 2011
Available online 13 October 2011

Keywords:
Quaternized
Poly(vinyl alcohol)
Silica
Anion-exchange membrane
Composite
Alkaline direct methanol fuel cell

ABSTRACT

The quaternized poly(vinyl alcohol)/3-(trimethyl ammonium) propyl-functionalized silica (designated as QPVA/Q-SiO_2) composite polymer membrane is prepared by a solution casting method. The Q-PVA is polyvinyl alcohol (PVA) derivatized with glycidytrimethyl ammonium chloride (GTMAC) and the Q-SiO_2 is 3-(trimethyl ammonium) propyl-functionalized silica. The highest ionic conductivity of the QPVA/20 wt.%Q-SiO_2 composite polymer electrolyte is $\sigma = 2.37\,mS\,cm^{-1}$ at ambient temperature. The alkaline direct methanol fuel cell (ADMFC) comprised of an anion-exchange QPVA/Q-SiO_2 composite membrane is assembled and examined. The highest peak power density of the DMFC with 8 M KOH + 2 M CH_3OH fuel is $35.13\,mW\,cm^{-2}$ at 50 °C and 1 atm air. The peak power density is $0.27\,mW\,cm^{-2}$ with a pure 2 M CH_3OH fuel at 25 °C and 1 atm air.

1. Introduction

The DMFCs have recently attracted significant attention for their potential applications on electric vehicles (EVs), stationary applications, and portable power sources, such as cellular phones, and notebook computers, etc. The direct methanol fuel cell (DMFC) is being actively studied and significant progress has been made over the past few years [1–15]. However, the development of the DMFC has been hampered due to several problems, such as slow methanol oxidation kinetics and incomplete electrooxidation of methanol, the poisoning of adsorbed intermediate species on the Pt surface, the high methanol crossover through the solid-state polymer Nafion membrane, and the high costs of the Nafion (Du Pont) polymer membrane and Pt catalyst.

Yang [1,2] synthesized the crosslinked PVA-based composite polymer membranes and applied them in an alkaline DMFC. The carbonation problem of alkaline DMFC can be significantly reduced by using an alkaline solid polymer membrane instead of an alkaline solution [3–6]. In addition, the anodic electrooxidation of methanol in an alkaline medium shows significantly faster kinetics than that in an acidic medium [7]. The works on the preparation of the anion exchange polymer membrane for alkaline DMFC have been studied intensively [8–15]. Several types of anion exchange polymer membrane based on quaternized polymers applied for alkaline alcohol fuel cells have recently been investigated [9,15].

Xiong et al. [16] studied a quaternized poly(vinyl alcohol) polymer membrane (QPVA) that is poly(vinyl alcohol) derivatized with glycidytrimethyl ammonium chloride (GTMAC) for applications in DMFC. The quaternary ammonium groups were grafted onto the backbone of the PVA host. The ionic conductivity of the QPVA exchange polymer membrane was $7.34 \times 10^{-3}\,S\,cm^{-1}$ in deionized water at 30 °C. Xiong et al. [17,18] also prepared and examined two organic–inorganic hybrid anion-exchange membranes based on QPVA and tetraethoxylsilanes (TEOS) [17] and QPVA/chitosan [18]. These composite polymer membranes show a high ionic conductivity of 10^{-3} to $10^{-2}\,S\,cm^{-1}$ and a low methanol permeability of 5.68×10^{-7} to $4.42 \times 10^{-6}\,cm^2\,s^{-1}$ at 30 °C. However, they did not show any electrochemical data for applications in an alkaline DMFC [16–18].

Several ceramic fillers are being used on the polymer electrolyte membrane, for examples, TiO_2 [1], SiO_2 [6], α-Al_2O_3 [19], and bentonite [20], which are blended into the PVA polymer. Yang et al. [21] recently prepared and studied QPVA/Al_2O_3 composite polymer membranes on alkaline DMFCs. Wang et al. [22] prepared a hybrid polymer membrane for an alkaline direct ethanol fuel cell (DEFC) based on PVA and 3-(trimethyl ammonium) propyl-functionalized silica (denoted as Q-SiO_2). The highest peak power density of DEFC with an alkaline composite hybrid membrane is $50\,mW\,cm^{-2}$ at 60 °C. Silica (SiO_2) was used due to its good physical and chemical properties. Silica is typically used in the form of nano-particles, which provide high surface area and activity,

* Corresponding author. Tel.: +886 29089899; fax: +886 29041914.
E-mail address: ccyang@mail.mcut.edu.tw (C.-C. Yang).

0378-7753/$ – see front matter © 2011 Elsevier B.V. All rights reserved.
doi:10.1016/j.jpowsour.2011.10.020

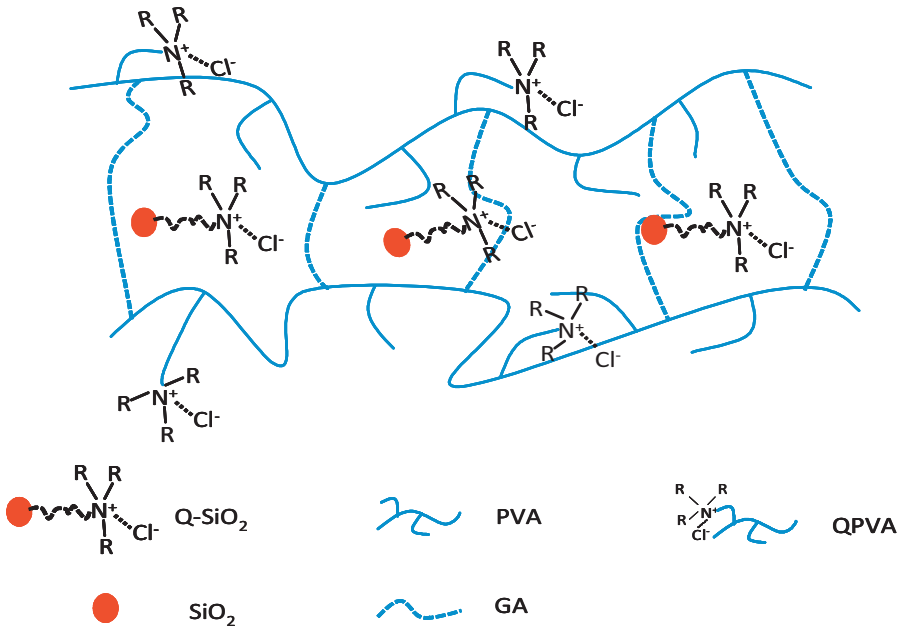

Fig. 1. A schematic diagram of the structure of a crosslinked QPVA/Q-SiO2 (or TMAPFS) composite membrane.

and excellent chemical stability. The addition of hydrophilic SiO_2 fillers into the polymer matrix reduces the crystallinity of the PVA polymer, therefore increasing the amorphous phases of the PVA polymer matrix, resulting in an increase of its ionic conductivity. When Q-SiO_2 filler is used as an ionic functional material and added to the PVA matrix, the ionic conductivity properties of the QPVA/Q-SiO_2 composite polymer membrane is significantly enhanced. The thermal property, dimensional stability, and swelling ratio may also be improved.

In this study, we attempt to add 3-(trimethyl ammonium) propyl-functionalized SiO_2 (that is, Q-SiO_2) into the QPVA matrix, to act as the ionic source and solid plasticizer which is capable of enhancing the ionic conductivity, the chemical and thermal properties, and the dimensional stability for the QPVA/Q-SiO_2 composite polymer membrane. Alkaline DMFC, comprised of the air cathode loaded with MnO_2/BP2000 carbon ink on a Ni-foam, the PtRu anode based on a Ti-screen, and QPVA/Q-SiO_2 composite polymer membrane, was assembled and investigated. The QPVA/Q-SiO_2 composite polymer membrane was prepared by a direct blend of QPVA polymer (PVA being amination by GTMAC first) and Q-SiO_2 fillers under continuous stirring. A 5 wt.% glutaraldehyde (GA) solution was directly added to the composite polymer membrane for the crosslinking reaction. The electrochemical characteristics of alkaline DMFC comprised of QPVA/Q-SiO_2 composite polymer membrane were investigated by the linear polarization and galvanostatic methods; especially for the peak power density of alkaline DMFC at ambient conditions.

2. Experimental

2.1. Preparation of the QPVA/Q-SiO_2 composite membrane

The PVA (average molecular weight of 89,000–98,000, more than 99% hydrolyzed, Aldrich), 3-(trimethyl ammonium) propyl-functionalized silica (Q-SiO_2) (Aldrich), glycidytrimethyl ammonium chloride (GTMAC) (Aldrich), and KOH (Merck) were used without further purification. The QPVA/Q-SiO_2 composite polymer membrane was prepared by a solution casting method [21].

The appropriate quantities of the PVA polymer were dissolved in distilled water under stirring. The resulting solution was stirred until the solution mixture became homogeneous with a viscous appearance at 85 °C for 3 h. The temperature of the viscous mixture was cooled to 65 °C, after which an appropriate amount of GTMAC, KOH (GTMAC:KOH = 1:1 in a molar ratio) was added to the resulting mixture solution under a continuous stirring condition for 4 h. The resulting viscous polymer mixture was washed with anhydrous alcohol to obtain yellow precipitates. Then, these quaternized poly(vinyl alcohol) precipitates (denoted as QPVA) were then dried at 65 °C in a vacuum oven.

The QPVA/Q-SiO_2 mixture solution was prepared by using a suitable amount of as-prepared QPVA precipitates, 0–20 wt.%Q-SiO_2 fillers, and 5 wt.%GA (a cross linking agent), 1 vol.% HCl at 85 °C for 3 h under a continuous stirring condition. The resulting viscous blend polymer solution was poured onto a glass plate. The thickness of the wet composite polymer membrane was between 0.020 and 0.040 cm. The thickness of the dried composite polymer membrane was controlled in the range of between 0.010 and 0.020 cm. Fig. 1 shows a schematic diagram for the structure of a cross-linked QPVA/Q-SiO_2 composite membrane.

2.2. Crystal structure, morphology, and thermal analyses

TGA thermal analysis was conducted by using a Mettler Toledo TGA/SDT 851 system. Te measurements were conducted by heating from 25 to 600 °C, under N_2 atmosphere at a heating rate of 10 °C min^{-1} with approximately 10 mg samples. The surface morphology and microstructure of the QPVA/Q-SiO_2 composite polymer membrane were investigated by a scanning electron microscope (SEM) (Hitachi S-2600H).

2.3. Ionic conductivity, ion-exchange capacity, and methanol permeability measurements

The conductivity measurements of QPVA/Q-SiO_2 composite electrolytes were conducted via an AC impedance method. The composite samples were first immersed in a 1 M KOH solution for 24 h for ionic exchange, washed several times by D.I. water, finally dipped in D.I. water for 12 h for further testing. The QPVA/Q-SiO_2 composite anion-exchange membranes were clamped between stainless steel (SS304), as ion-blocking electrodes, each with a

surface area 1.32 cm^2, in a spring-loaded glass holder. A thermocouple was maintained in close proximity to the composite polymer membrane for temperature measurement. Each sample was equilibrated at the experimental temperature for a minimum of 30 min prior to measurement. The AC impedance measurements were conducted by using an Autolab PGSTAT-30 equipment (Eco Chemie B.V., Netherlands). The AC spectra in the range of 100 kHz to 100 Hz at an excitation signal of 10 mV were recorded. AC impedance spectra of the composite anion-exchange membrane were recorded at a temperature range between 30 and 70 °C. The experimental temperatures were maintained within ±0.5 °C in a convection oven. All composite polymer electrolytes were examined a minimum of three times. The ion-exchange capacity (IEC), defined as mmol g^{-1}, was examined by using the standard back-titration technique [12–14].

The methanol permeability measurements [23,24] were conducted by using a diffusion cell. The cell was divided into two compartments, one of which was filled with D.I. water (called B compartment) and the other filled with a 20 wt.% methanol aqueous solution (called A compartment). The QPVA/Q-SiO_2 composite polymer membrane was hydrated in D.I. water for at least 24 h prior to testing. The composite polymer membrane with a surface area of 0.58 cm^2 was sandwiched by O-ring and clamped tightly between two compartments. A stir bar was kept active in the glass diffusion cell during the experiment. The concentration of the methanol diffused from compartment A to B across the composite polymer membrane was examined by using a density meter (Mettler Toledo, DE45). An aliquot of 0.20 mL was sampled from the B compartments every 30 min. A calibration curve for the value of density vs. the methanol concentration was prepared prior to the permeation experiment. The calibration curve was used to calculate the methanol concentration in the permeation experiment. The methanol permeability was calculated from the slope of the straight-line plot of methanol concentration vs. permeation time. The methanol concentration in the B compartment as a function of time is given in Eq. (1) [23]:

$$C_B(t) = \frac{A}{V}\frac{DK}{L}C_A(t - t_0) \quad (1)$$

where C is the methanol concentration, A and L are the composite membrane area and thickness; and D and K are the methanol diffusivity and partition coefficient between the membrane and the solution. The product DK is the membrane permeability (P), t_0, a time lag, is related to the diffusivity (D): $t_0 = L^2/6D$.

2.4. Micro-Raman spectroscopy analyses and nitrogen contents analyses

Micro-Raman spectroscopy is a tool that is used to quickly characterize pure PVA and the QPVA and QPVA/Q-SiO_2 composite polymer membranes. The micro-Raman spectroscopy analysis was conducted by using a Renishaw confocal microscopy Raman spectroscopy system with a microscope equipped with a 50× objective, and a charge coupled device (CCD) detector. Raman excitation source was provided by a 632.8 nm He–Ne laser beam, which had the beam power of 17 mW and was focused on the sample with a spot size of approximately 1 μm in a diameter. The N content in the sample was analyzed by using an Elemental Analyzer (Perkin Elmer 2400).

2.5. Preparation of the anode and cathode electrodes

The catalyst slurry ink for the anode was prepared by mixing 70 wt.% PtRu black inks (Alfa, HiSPEC 6000, PtRu black with Pt:Ru = 1:1 at. ratio), 30 wt.% PTFE binder solution (Du Pont, 60 wt.% base solution), and a suitable amount of distilled water and alcohol. The resulting PtRu black mixtures were ultrasonicated for 2 h. The PtRu black inks for the anode were loaded onto a Ti-screen [1,10] by an impregnation method, which was loaded with 4 mg cm^{-2}. The as-prepared PtRu anode was dried in a vacuum oven at 110 °C for 2 h.

The carbon slurry for the gas diffusion layer of the air cathode was prepared with a mixture of 70 wt.% Shawinigan acetylene black (AB50) with a specific surface area of 80 $m^2\ g^{-1}$ and 30 wt.% PTFE solution (Teflon-30 suspension) as a wet-proofing agent and binder. The carbon slurry was coated on the Ni-foam that was used as a current collector, and then pressed at 100 $kg_f\ cm^{-2}$. The gas diffusion layer was then sintered at a temperature of 360 °C for 30 min. The catalyst layer of the air cathode was then prepared by spraying a mixture of a 15 wt.% of PTFE binder and 85 wt.% of mixed powders consisting of MnO_2 catalyst mixed with BP2000 carbon black (MnO_2:BP2000 = 1:1). The MnO_2/C catalyst loading on the cathode was controlled at 4 mg cm^{-2}. The Ni-foam current collector was 1 cm × 1 cm. The detailed preparation method of the air electrodes has been reported in the literature [21,25].

2.6. Electrochemical measurements

The QPVA/Q-SiO_2 anion-exchange composite membrane was "sandwiched" between the sheets of the anode and the cathode, and then pressed at 25 °C under 100 $kg_f\ cm^{-2}$ for 5 min to obtain a membrane electrode assembly (MEA). The electrode area of the MEA was approximately 1 cm^2.

The electrochemical measurements of alkaline DMFC were carried out in a two-electrode system. The polarization (I–V) and the power density curves of alkaline DMFC consisting of QPVA/Q-SiO_2 composite anion-exchange membrane with 1–8 M KOH + 2 M CH_3OH solution or pure 2 M CH_3OH fuel were recorded at 25 and 50 °C. All electrochemical measurements were performed on an Autolab PGSTAT-30 electrochemical system with GPES 4.8

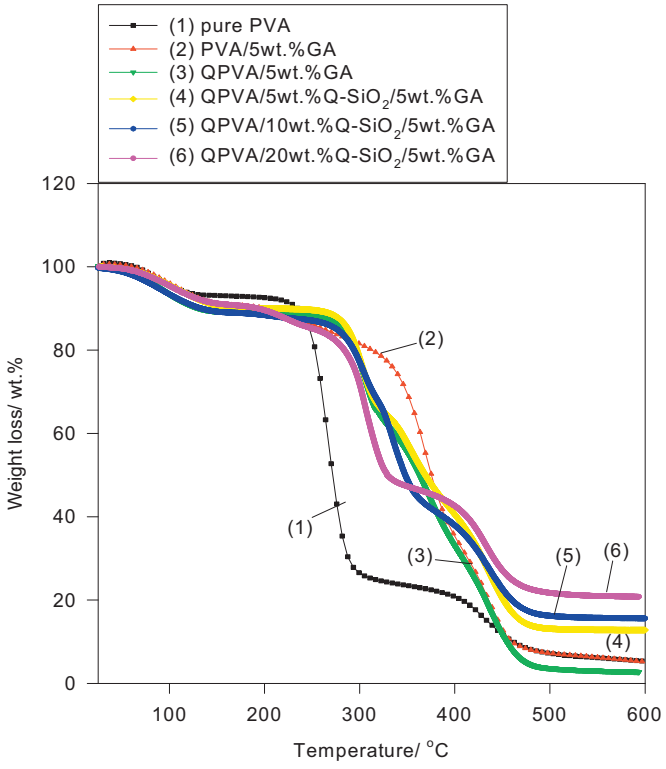

Fig. 2. TGA thermograph for the QPVA/x wt.%Q-SiO2/5 wt.%GA composite polymer membranes.

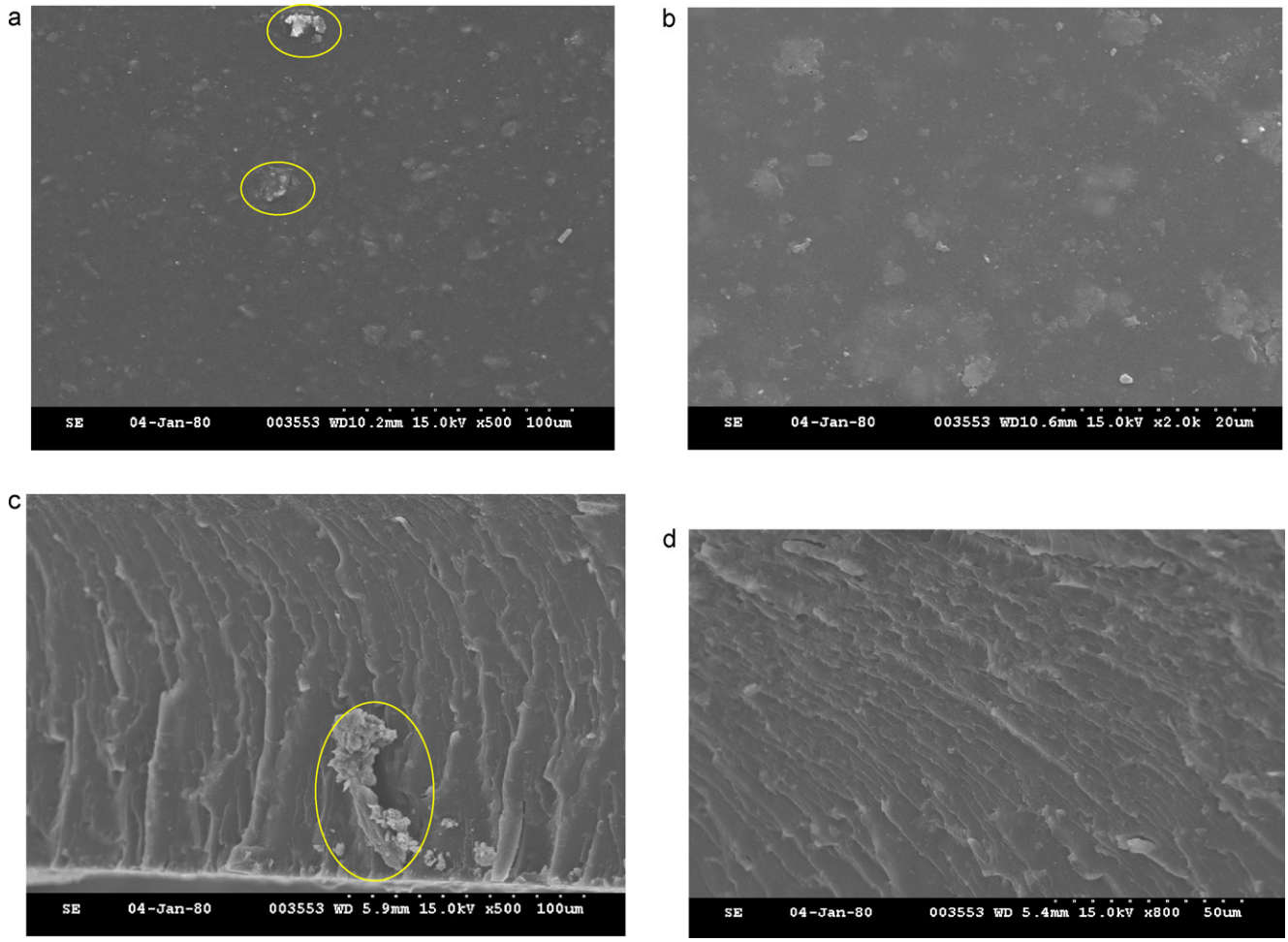

Fig. 3. SEM images for the QPVA/20 wt.%Q-SiO2/5 wt.%GA SPE: the top views (a and b); the cross-section views (c and d); the aggregates indicated by the circles.

package software (Eco Chemie, The Netherlands). The electrochemical performances of alkaline DMFC comprised of a QPVA/Q-SiO_2 anion-exchange composite membrane and the cathode open to atmospheric air were systematically studied at room temperature and in ambient air [1,2].

3. Results and discussion

3.1. Thermal analyses

Fig. 2 shows TGA curves for pure PVA film, the QPVA film and the QPVA/Q-SiO_2 composite membrane, respectively. The TGA curve of pure PVA film shows three major weight loss regions. The first region at a temperature of 80–130 °C ($T_{max,1}$ = 89.1 °C) is due to the evaporation of the weak physical and strong chemically bound H_2O; and the weight loss of the membrane is approximately 5–6 wt.%. The second transition region at approximately 240–310 °C ($T_{max,2}$ = 264 °C) is due to the degradation of the PVA polymer membrane; and the total weight loss corresponds to this phase, which is approximately 60–70 wt.%. The peak of third stage at approximately 410–460 °C ($T_{max,3}$ = 439 °C) is due to the cleavage backbone of PVA polymer film; and the total weight loss is approximately 94.63 wt.% at 600 °C.

Fig. 2 also shows TGA curves of the QPVA polymer membrane. The QPVA film also shows three major weight loss regions. In the QPVA film, the first region, at a temperature of 80–150 °C ($T_{max,1}$ = 89.2 °C), is due to the evaporation of the weak physical and strong chemically bound water; and the weight loss of the membrane is also approximately 6–7 wt.%. The peak of the second transition, at approximately 250–320 °C ($T_{max,3}$ = 270 °C), is due to the degradation of the PVA polymer membrane. The peak of third stage, at 410–470 °C ($T_{max,4}$ = 445 °C), is due to the cleavage of the C–C backbone of QPVA polymer membranes; and the total weight loss is approximately 94.33 wt.% at 600 °C.

The TGA curve of the QPVA/5–20 wt.%Q-SiO_2 composite polymer membrane also reveals three major weight loss regions, which appear as three peaks in the DTG curves. The first region, at a temperature of 80–150 °C ($T_{max,1}$ = 83 °C), is also due to the evaporation of the free and bound H_2O; and the weight loss of the membrane is ~5 wt.%. The peak of the second transition, at approximately 220–280 °C ($T_{max,3}$ = 246 °C), is also due to the degradation of the QPVA polymer membrane. The peak of the third transition, at 420–480 °C ($T_{max,4}$ = 440 °C), is due to the cleavage of the C–C backbone of the QPVA polymer membrane; and the total weight loss is approximately 77 wt.% at 600 °C.

Accordingly, the degradation peaks of crosslinked QPVA/Q-SiO_2 composite membranes are less intense and shift towards higher temperatures. It is concluded that the thermal stability may be improved due to the additive effect of Q-SiO_2 fillers and the chemical cross-link reaction between QPVA and glutaraldehyde (GA).

3.2. Surface morphology, mechanical properties, and micro-Raman analyses

The SEM photographs of the top and cross-section views of the QPVA/20 wt.%Q-SiO_2 composite membranes are shown in

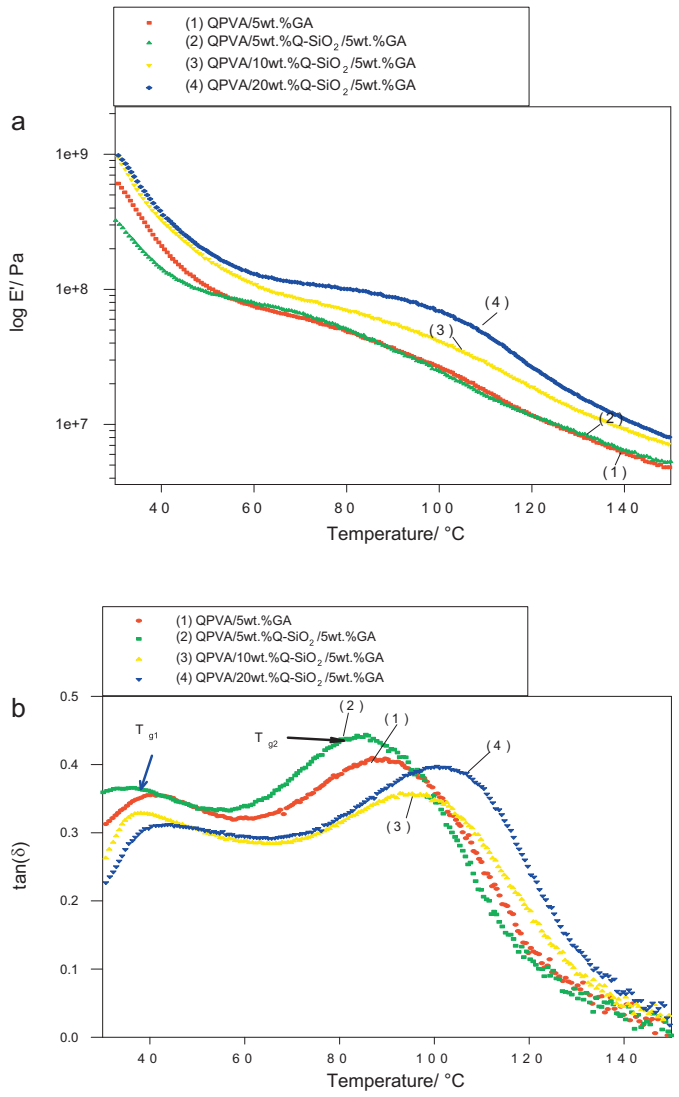

Fig. 4. DMA curves for the PVA, QPVA/*x* wt.%Q-SiO2 composites SPEs: (a) E' vs. T and (b) tan(δ) vs. T.

Fig. 3(a)–(d), respectively. It is revealed that the surface morphology of the QPVA/20 wt.%Q-SiO_2 composite sample shows a number of Q-SiO_2 aggregates or chunks, which are randomly distributed on the top surface. It is found that the dimension of these Q-SiO_2 aggregates, embedded in PVA matrix, is approximately 5–10 μm, as shown in Fig. 3(a) and (c), which indicated by the yellow circle. The SEM results indicate that the nano-sized Q-SiO_2 fillers tend to cause the formation of a number of aggregates, and thus cause a dispersion problem in the PVA polymer host. (For interpretation of the references to color in this paragraph, the reader is referred to the web version of the article.)

Accordingly, the hydrophilic PVA polymer and Q-SiO_2 fillers are homogeneous and compatible without the occurrence of any phase separation occurred when a suitable amount of Q-SiO_2 fillers are added. The appropriate amount of Q-SiO_2 fillers (used as the ionic source and the methanol permeation barrier) in the polymer network matrix may assist in increasing the ionic conductivity and reducing methanol crossover through the composite anion-exchange membrane.

Fig. 4(a) shows the storage modulus (E') vs. temperature curves for pure PVA film, QPVA film, and QPVA/*x* wt.%Q-SiO_2 composite membrane. The storage modulus, E', reflects the stiffness and the strength of the composite polymer and is a measure of the maximum storage energy of the composite polymer in one oscillation's cycle. The storage modulus of pure PVA film ($E' = 1.13 \times 10^9$ Pa) was higher than those of QPVA film ($E' = 1.44 \times 10^8$ Pa) and QPVA/10 wt.%Q-SiO_2 composite polymer membrane ($E' = 5.99 \times 10^8$ Pa) at 30 °C [26,27]. It was demonstrated that the storage moduli of QPVA film and QPVA/Q-SiO_2 composite membranes decrease when the Q-SiO_2 fillers are added or when the PVA polymer is being quaternized by GTMAC. The hydroxyl groups of PVA polymer generally contribute to the stiffness of the linear polymer. When the number of hydroxyl groups decreases by quaternized branching or GA crosslinking, the hydrogen bonding is decreased and thus the chain stiffness is attenuated, i.e. E' decease. In fact, the storage modulus of the QPVA/20 wt.%Q-SiO_2 composite membrane at 100 °C ($E' = 1.72 \times 10^8$ Pa) was higher than that of pure PVA film ($E' = 1.51 \times 10^8$ Pa). This increase is attributed to the introduction of Q-SiO_2 into QPVA matrix. Due to rigidity of Q-SiO_2 ceramic fillers, the composite membrane becomes more rigid when the amount of Q-SiO_2 fillers increases.

It was confirmed that these functional silica fillers significantly enhanced the mechanical properties of the QPVA/Q-SiO_2 composite membrane. However, when the content of Q-SiO_2 fillers was above 20 wt.%, the stiffening effect was progressively decreased due to the significant agglomeration of Q-SiO_2 fillers in the PVA polymer host.

Fig. 4(b) shows the loss factor or tan(δ) vs. temperature curves for the pure PVA film, the QPVA film, and the QPVA/*x* wt.%Q-SiO_2 composite membranes. The glass transition temperatures (T_g) can also be recorded at a peak of the tan(δ) curve (denoted as tan$(\delta)_1$). The tan(δ), which is the ratio of E''/E', is a measure of how close the composite polymer is to the ideal elastic behavior. Higher the tan(δ), the higher the viscoelasticity of the composite polymer and thus the better the ability survive the cycling stress. The results indicate that the glass transition temperatures of pure PVA film (designated as a $T_{g,\,PVA}$) and the QPVA/20 wt.%Q-SiO$_2$ SPE are 30.87 °C and 41.25 °C, respectively. The glass transition temperatures of the QPVA film and the QPVA/20 wt.%Q-SiO_2 SPE (approximately 37–41 °C) are higher than that of pure PVA film (at 30.8 °C). Generally, the sensitivity of the glass transition temperature measurement by DMA is superior to that by DSC. It may be concluded that the actual glass transition temperature of the QPVA/20 wt.%Q-SiO_2 composite membrane is approximately 37–41 °C. The quaternized PVA polymer films (that is, QPVA and QPVA/Q-SiO_2) show significantly stiffer properties, as compared with pure PVA film.

It was also observed that there are two tan(δ) peaks, tan$(\delta)_1$ and tan$(\delta)_2$, for the QPVA/20 wt.%Q-SiO_2 composite polymer membranes; the variation region of the first tan(δ) peak (take tan$(\delta)_1$ as $T_{g,\,PVA}$ at 41.25 °C) is located between 20 and 60 °C. However, the secondary tan(δ) peak (designated as tan$(\delta)_2$) is observed at 101.09 °C, the so-called β_c relaxation; and is due to the relaxation of the crystalline domain of QPVA/20 wt.%Q-SiO_2 composite membrane. A clear tan$(\delta)_2$ peak could nor be observed on pure PVA film. It was revealed that the degree of crystallinity of the QPVA/20 wt.%Q-SiO_2 SPE is higher than that of the QPVA SPE.

Fig. 5(a) shows the micro-Raman spectra of GTMAC (used as an animating agent), pure PVA film, and the QPVA film. Several strong characteristic scattering peaks for the pure PVA film are located at 852, 918, 1140, 1440 cm^{-1}. It can be observed from the micro-Raman spectra that a number of characteristic peaks for GTMAC are found at 760, 867, 897, 940, 1265, 1443 cm^{-1}. In contrast, there are several main peaks for the QPVA film, located at 760, 852, 883, 926, 1081, 1088, 1145, 1362, 1440 cm^{-1}, as seen in Fig. 5(a). In particular, three additional Raman characteristic peaks at 760, 883, and 1265 cm^{-1} appeared on the QPVA film, as compared with the Raman peaks of pure PVA. The peak at 760 cm^{-1} is due to the C–N stretching; the peak at 883 cm^{-1} is identified for C–O–C stretching; and the peak of 1265 cm^{-1} could be due to the C–H deformation.

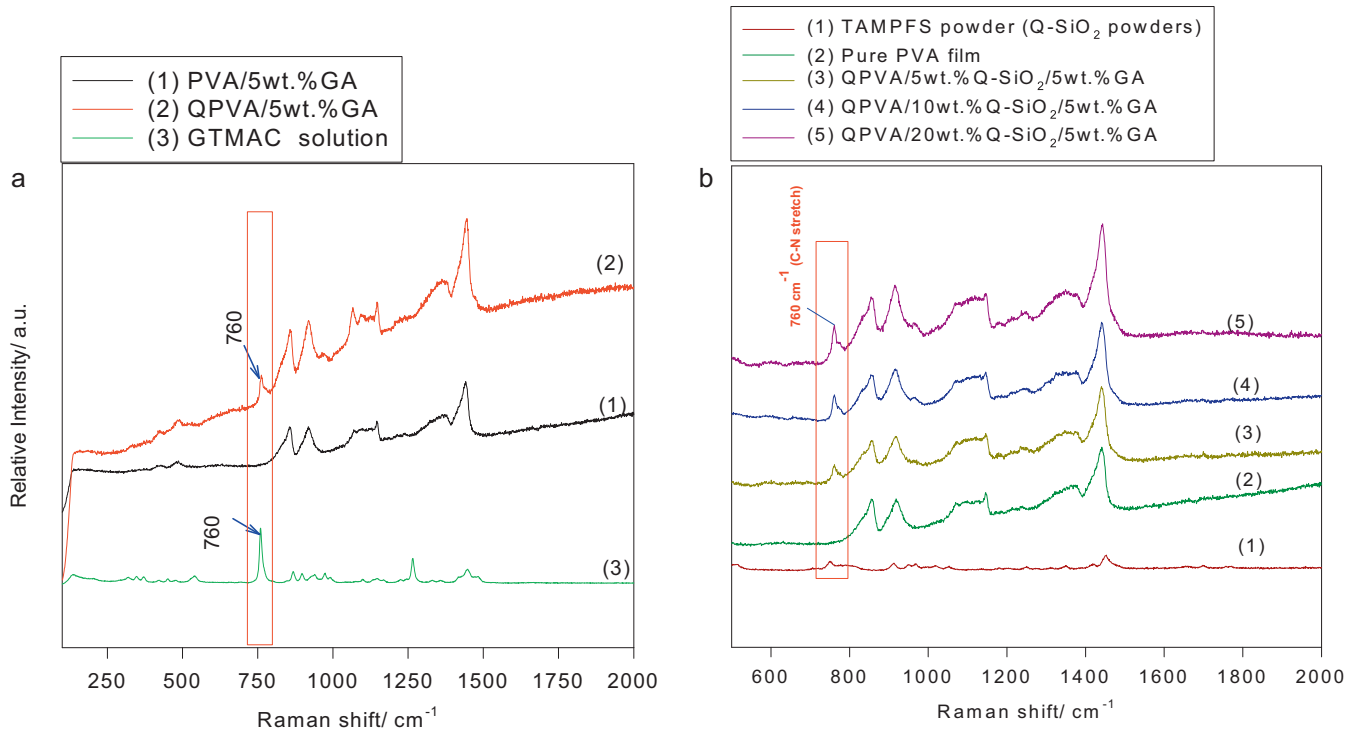

Fig. 5. Micro-Raman spectra for (a) PVA, GPTMAC solution, and QPVA. (b) TAMPFS (donated as Q-SiO2) fillers and the QPVA/*x* wt.%Q-SiO2/5 wt.%GA SPEs.

Table 1
Assignments for major Raman peaks of QPVA/Q-SiO_2 composite membranes.

Frequency/cm^{-1}	Assignment for scattering bonds
760	C–N stretching (GTMAC or TMAPFS)
852	C–C stretching (QPVA)
926	C–C stretching (QPVA)
1081	C–C stretching, O–H bending (QPVA)
1088	C–C stretching, O–H bending (QPVA)
1145	C–C stretching, C–O stretching (QPVA)
1362	C–H bending, O–H bending (QPVA)
1440	C–H bending, O–H bending (QPVA)

This proves that PVA polymer has been successfully quaternized by GTMAC via a quaternization process. Fig. 5(b) shows the micro-Raman spectra of the QPVA/*x* wt.%Q-SiO_2 composite membranes at various compositions of Q-SiO_2 fillers. Table 1 lists several major Raman peak positions for GTMAC, the pure PVA film, the QPVA film, and the QPVA/Q-SiO_2 composite membranes.

3.3. Ionic conductivity, IEC, and methanol permeability

The typical AC impedance spectra of the QPVA/20 wt.%Q-SiO_2 composite membrane at various temperatures are shown in Fig. 6(a). The AC spectra were typically non-vertical spikes for stainless steel (SS) blocking electrodes (that is, the SS|QPVA/Q-SiO_2 SPE|SS cell). An analysis of the spectra yielded information about the properties of the QPVA/Q-SiO_2 composite polymer electrolyte, such as bulk resistance, R_b. Taking into account the thickness of the nanocomposite electrolyte films, the R_b value was converted into the ionic conductivity value, σ, according to the equation: $\sigma = L/R_bA$, where L is the thickness (cm) of QPVA/Q-SiO_2 composite membrane, A is the area (cm^2) of the blocking electrode, and R_b is the bulk resistance (ohm) of the alkaline composite membrane electrolyte.

Typically, the R_b values of QPVA/20 wt.%Q-SiO_2 composite membranes are in the order of 0.2–0.3 Ω and are highly dependent on the contents of Q-SiO_2 fillers and the concentration of KOH. The anion-exchange composite membrane was immersed in a 1 M KOH solution for 24 h for ionic exchange, and then washed several times with D.I. water.

Table 2 lists the ionic conductivity values of the pure PVA film, the QPVA film, and QPVA/20 wt.%Q-SiO_2 composite membrane with D.I. water at various temperatures. As a result, the ionic conductivity of the pure PVA film is 0.039 mS cm^{-1} at 30 °C. Comparatively, the ionic conductivities of QPVA/5 wt.%Q-SiO_2, QPVA/10 wt.%Q-SiO_2, and QPVA/5 wt.%Q-SiO_2 anionic-exchange composite membranes are 1.30, 1.45, and 2.37 mS cm^{-1} at 30 °C, respectively. It was observed that the highest ionic conductivity of the QPVA/20 wt.%Q-SiO_2 composite membrane electrolyte is σ = 2.37 mS cm^{-1} at ambient temperature. It was also found that the ionic conductivity of the QPVA film (σ_{30oc} = 1.24 mS cm^{-1}) is higher than that of the pure PVA film (σ_{30oc} = 0.039 mS cm^{-1}) [21]. The ionic conductivity of pure PVA membrane in water is the order

Table 2
Ionic conductivities of QPVA/*x* wt.%Q-SiO_2/5 wt.%GA composite membranes in D.I. water at various temperatures.

Temp.	σ/mS cm^{-1}				
	PVA/5 wt.%GA	QPVA/5 wt.%GA	QPVA/5 wt.%Q-SiO_2/5 wt.%GA	QPVA/10 wt.%Q-SiO_2/5 wt.%GA	QPVA/20 wt.%Q-SiO_2/5 wt.%GA
30 °C	0.039	1.24	1.30	1.45	2.37
40 °C	0.054	1.50	1.57	1.80	2.82
50 °C	0.069	1.85	1.94	2.31	3.45
60 °C	0.084	2.25	2.38	3.00	4.67
70 °C	0.098	2.64	2.74	3.70	6.40

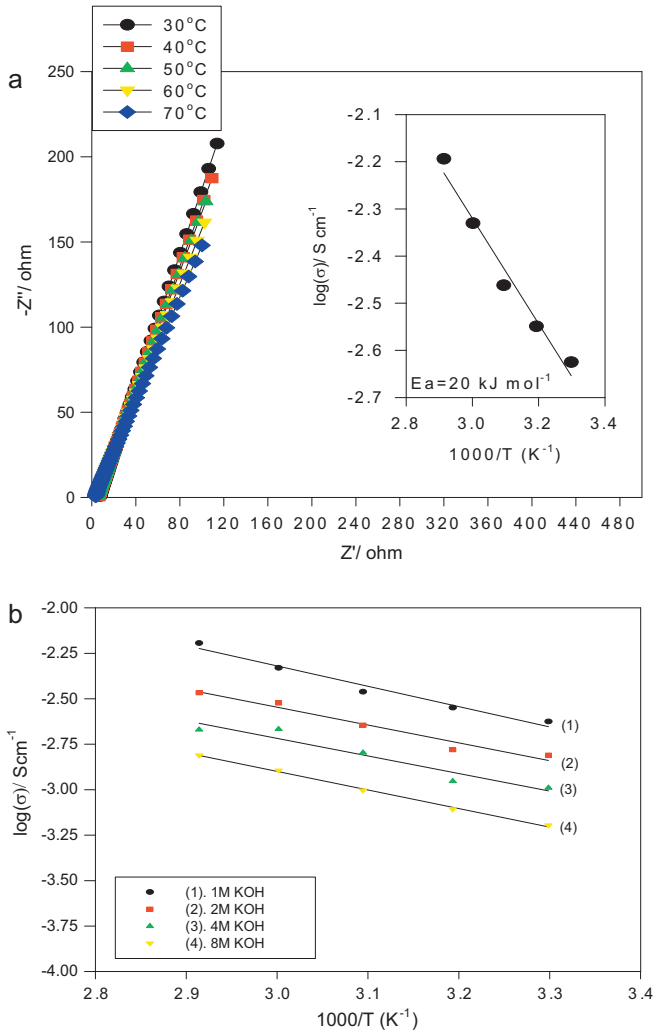

Fig. 6. (a) Nyquist plot and Arrhenius plot (inset) for QPVA/20%Q-SiO2 SPE in D.I. water and (b) Arrhenius plot for QPVA/20%Q-SiO2 SPE by *x* M KOH for ionic exchange.

of 10^{-5} S cm^{-1} at 30 °C, but the ionic conductivities of QPVA and QPVA/Q-SiO_2 composite polymer membranes in water are about 10^{-3} S cm^{-1}. It can be observed clearly that there is a two order magnitude difference. Comparatively, the ionic conductivities of the pure PVA membrane, QPVA membrane, QPVAQ-SiO_2 composite polymer electrolyte membranes containing with free KOH electrolyte are all of order of 10^{-1}–10^{-2} S cm^{-1} at room temperature [1,2,28]. The higher the ionic conductivity of the composite polymer electrolyte membranes; the ohmic loss (or IR drop) on DMFC can be greatly reduced during the operation period. It can be seen clearly that the KOH electrolyte plays an important role in improving the ionic conductivity of polymer electrolyte membranes.

According to the ionic conductivity result, it is observed that the ionic conductivity of the QPVA/Q-SiO_2 composite membrane electrolytes increases when the content of Q-SiO_2 fillers increase. When the Q-SiO_2 fillers with the quaternized functional groups (–$(CH_3)_3N^+$–) used as the ionic source and solid plastizer materials were added to the QPVA matrix. The ionic conductivity of QPVA/Q-SiO_2 composite electrolyte membranes increased from 1.24 (0%Q-SiO_2) to 2.37 (20 wt.%Q-SiO_2) mS cm^{-1} at 30 °C. It is because the Q-SiO_2 fillers contain quaternary ammonium (–N^+Me_3) ionic groups on SiO_2 fillers, not pure inert ceramic fillers. On the contrary, the swelling ratio of QPVA/Q-SiO_2 composite membrane reduced from 106% (0%Q-SiO_2) to 81.87% (20 wt.%Q-SiO_2). It is due to the increasing stiffness of the composite polymer membrane when the more Q-SiO_2 filler is added into the PVA matrix. The nitrogen (N) content in the composite polymer membrane was analyzed by elemental analyzer (EA). It was found that the QPVA/Q-SiO_2 anion-exchange composite membranes is in the range of 1.17–1.80%, as listed in Table 3. In general, the N content increased when the added amounts of Q-SiO_2 fillers increased. The ionic conductivity of the QPVA/Q-SiO_2 anionic-exchange composite membranes also increased when the N content in the samples increased [1,2,21]. Table 3 also shows the IEC data for the QPVA/0–20 wt.%Q-SiO_2 anion-exchange composite membranes; which varied from 0.41 to 0.635 mequiv. g^{-1}. The higher the value of IEC, the higher value of the ionic conductivity of the sample.

Table 3
The N content in the QPVA/*x* wt.%Q-SiO_2/5 wt.%GA SPEs.

Samples	Avg. N/%	IEC/mequiv. g^{-1}
TMAPS powder	3.15 ± 0.02	–
QPVA/5 wt.%GA	1.17 ± 0.03	0.410 ± 0.004
QPVA/5 wt.%Q-SiO_2/5 wt.%GA	1.31 ± 0.01	0.450 ± 0.002
QPVA/10 wt.%Q-SiO_2/5 wt.%GA	1.46 ± 0.03	0.502 ± 0.003
QPVA/20 wt.%Q-SiO_2/5 wt.%GA	1.84 ± 0.03	0.635 ± 0.003

As expected, the thermal and mechanical properties, and the dimensional stability also improved. The liquid uptake for D.I. water decreased from 50.18% to 45.01% when the amount of Q-SiO_2 fillers added in the QPVA/Q-SiO_2 composite membranes was increased from 5 wt.% to 20 wt.%. The swelling ratio in D.I. water simultaneously decreased from 100.7% to 81.9% when the amount of Q-SiO_2 fillers was increased from 5 wt.% to 20 wt.% (data not shown here).

However, the ionic conductivity of QPVA/Q-SiO_2 composite membrane electrolytes decreases when the content of Q-SiO_2 fillers is above 20 wt.%. According to the $\log_{10}(\sigma)$ vs. $1/T$ plots, as shown in the inset of Fig. 6(a), the activation energy (E_a) of the QPVA/20 wt.%Q-SiO_2 composite membrane electrolyte can be obtained, and is highly dependent on the contents of Q-SiO_2 fillers and KOH concentrations. In addition, the E_a value of the QPVA/5–20 wt.%Q-SiO_2 anionic-exchange composite membranes is in the order of 18–21 kJ mol^{-1}. The concentration of KOH electrolyte solution for the ionic exchange also significantly impacts on the ionic conductivity. As shown in Fig. 6(b), the QPVA/20 wt.%Q-SiO_2 anionic-exchange composite membrane in D.I. water showed the highest ionic conductivities at a temperature of 30–70 °C when 1 M KOH solution was used as the ionic exchange medium. The higher the KOH concentration used as the ionic exchange medium, the lower the value of the ionic conductivity.

The permeability measurements for methanol were carried out on the QPVA/Q-SiO_2 composite membrane. All values of methanol permeability for QPVA/Q-SiO_2 composite membranes were obtained from the slope of the straight line (also see Refs. [1,2]). It is revealed that the methanol permeability values of the QPVA/Q-SiO_2 composite membrane are 8.1×10^{-7}–5.41×10^{-7} cm^2 s^{-1}, at 25 °C. However, the permeabilities of the QPVA/Q-SiO_2 composite membranes (in the order of 10^{-7} cm^2 s^{-1}) are lower than that of the Nafion membrane (in the order of 10^{-6} cm^2 s^{-1}).

3.4. Electrochemical measurements

The potential–current density and the power density–current density curves of alkaline DMFCs with 1–8 M KOH + 2 M methanol fuels at 50 °C were obtained (not shown here). As a result, the highest peak power density of 35.13 mW cm^{-2} for the DMFC with a 8 M KOH + 2 M methanol fuel is achieved at $E_{p,max}$ = 0.280 V with a peak current density ($i_{p,max}$) of 125.34 mA cm^{-2}, as displayed in Table 4. Conversely, the peak power density of alkaline DMFC with a 4 M KOH + 2 M CH_3OH fuel is 30.10 mW cm^{-2} at $E_{p,max}$ = 0.27 V, with a

Table 4
The electrochemical parameters of alkaline DMFC (the anode: 4.0 mg cm^{-2} of PtRu black on Ti-screen) with QPVA/20 wt.%Q-SiO_2/5 wt.%GA composite membrane with 2 M methanol + *x* M KOH fuels at 50 °C and 1 atm air.

Fuel	Parm.			
	OCP/V	$i_{p,max}$/mA cm^{-2}	$E_{p,max}$/V	P.D.$_{max}$/mW cm^{-2}
1 M KOH + 2 M methanol	0.86	65.67	0.27	17.52
2 M KOH + 2 M methanol	0.85	79.90	0.26	20.91
4 M KOH + 2 M methanol	0.89	110.50	0.27	30.10
6 M KOH + 2 M methanol	0.90	126.95	0.27	34.29
8 M KOH + 2 M methanol	0.92	125.34	0.28	35.13

Table 5
The electrochemical parameters of alkaline DMFC (the anode: 4.0 mg cm^{-2} of PtRu black on Ti-screen) with three types alkaline composite membranes with 4 M KOH + 2 M methanol fuel at 25 °C and in ambient air.

Membrane	Parm.			
	OCP/V	$i_{p,max}$/mA cm^{-2}	$E_{p,max}$/V	P.D.$_{max}$/mW cm^{-2}
QPVA/20 wt.%Al_2O_3/5 wt.%GA [21]	0.90	76.90	0.24	18.33
PVA/5 wt.%SiO_2/5 wt.%GA [26]	0.90	50.75	0.26	13.10
QPVA/20 wt.%Q-SiO_2/5 wt.%GA [this work]	0.90	127.78	0.20	26.09

peak current density of 110.50 mA cm^{-2} at 25 °C. By comparison, the peak power density of the DMFC using a QPVA/20 wt.%Q-SiO_2 polymer membrane with a 4 M KOH + 2 M CH_3OH fuel (P.D.$_{max}$ = 26.09 mW cm^{-2}) is significantly higher than those of the DMFCs comprising of the QPVA/20 wt.%Al_2O_3 composite membrane (P.D.$_{max}$ = 18.33 mW cm^{-2}) [21] and the PVA/5 wt.%SiO_2 composite membrane (P.D.$_{max}$ = 19.57 mW cm^{-2}) at 25 °C [28] at the same amount of catalyst loadings on the electrodes (that is, the anode with 4 mg cm^{-2} PtRu black ink and the cathode with 4 mg cm^{-2} MnO_2/C ink), as shown in Fig. 7. The detailed electrochemical parameters of DMFCs with various compositions of alkaline composite membranes are summarized in Table 5 for comparison. It was shown clearly that the electrochemical performance, in terms of the peak power density, of DMFC with the QPVA/Q-SiO_2 composite polymer membrane (26.09 mW cm^{-2}) is superior to that of DMFC with the PVA/SiO_2 composite membrane (19.57 mW cm^{-2}).

This indicates that the electrochemical performance of DMFC comprised of alkaline polymer electrolyte membrane may be greatly improved through via by a quaternization process [8–10] on the polymer matrix and the addition of functionalized ceramic fillers.

Fig. 8 shows the potential–current density and the power density–current density curves of alkaline DMFCs comprising of the QPVA/20 wt.%Al_2O_3/5 wt.%GA and the QPVA/20 wt.

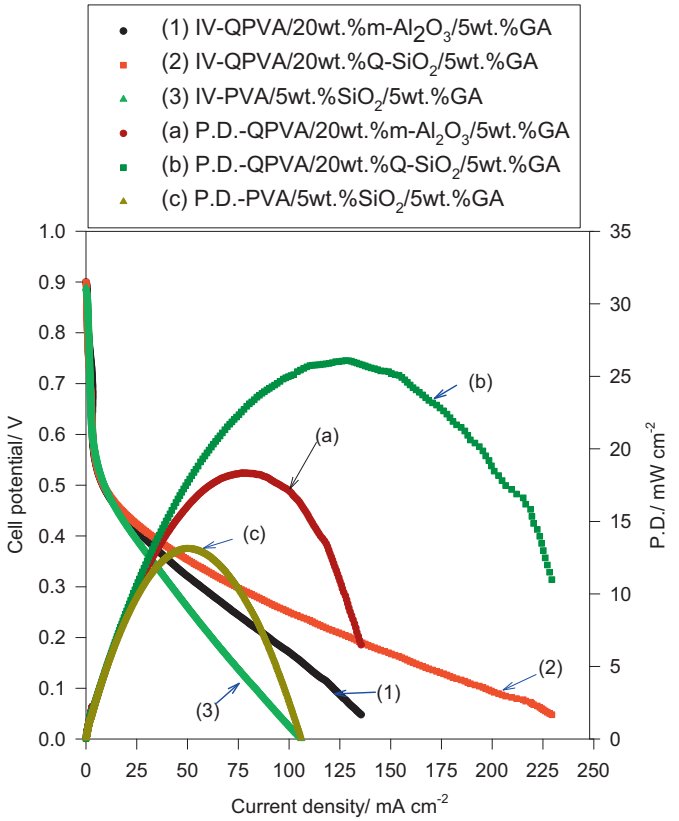

Fig. 7. The *IV* and P.D. curves of alkaline DMFCs with three types composite polymer membranes with a 4 M KOH + 2 M CH_3OH fuel for comparison (at 25 °C and 1 atm air).

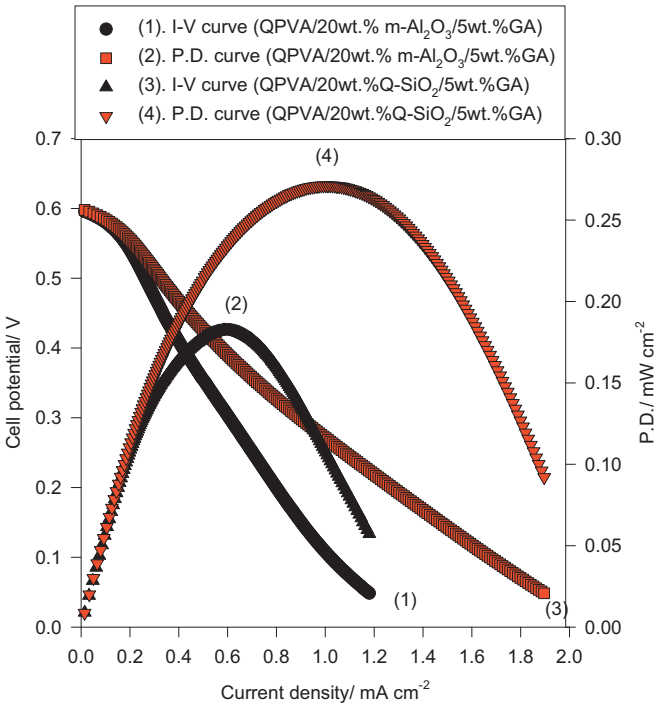

Fig. 8. Comparison of the *IV* and P.D. curves of the ADMFCs comprised of the QPVA/20 wt.%Q-SiO2/5 wt.%GA and the QPVA/20 wt.%m-Al2O3/5 wt.%GA SPEs using a pure 2 M MeOH fuel (25 °C and 1 atm air).

Table 6
The electrochemical parameters of alkaline DMFC (the anode: 4.0 mg cm^{-2} of PtRu black on Ti-screen) with two types anionic-exchange composite membranes with pure 2 M methanol fuel at 25 °C and in ambient air.

Membrane	Parm.			
	OCP/V	$i_{p,max}$/mA cm^{-2}	$E_{p,max}$/V	P.D.$_{max}$/mW cm^{-2}
QPVA/20 wt.%Al_2O_3/5 wt.%GA	0.61	0.58	0.31	0.18
QPVA/20 wt.%Q-SiO_2/5 wt.%GA	0.61	1.00	0.27	0.27
Ref. [29]	0.58	–	–	0.32

%Q-SiO_2/5 wt.%GA anion-exchange composite membranes with pure 2 M methanol fuel, at 25 °C and 1 atm air. As a result, the peak power density of 0.18 mW cm^{-2} for the DMFC with the QPVA/20 wt.%Al_2O_3/5 wt.%GA SPE is achieved at $E_{p,max}$ = 0.31 V with a peak current density ($i_{p,max}$) of 0.18 mA cm^{-2}. Conversely, the peak power density of alkaline DMFC with the QPVA/20 wt.%Q-SiO_2/5 wt.%GA SPE is 0.27 mW cm^{-2} at $E_{p,max}$ = 0.27 V with a peak current density of 1.00 mA cm^{-2} at 25 °C, as listed in Table 6. Santasalo et al. [29] recently studied anionic-exchange composite membrane (a new commercial fumasep FAA-2 membrane) on ADMFC using 1 M methanol. The cell showed E_{ocp} of 0.58 V and P.D. of 0.32 mW cm^{-2}.

Our P.D. data are comparable to their data of Santasalo et al. [29]. It was revealed that the peak power density value (P.D. = 0.27 mW cm^{-2}) of the ADMFC with pure 2 M methanol fuel was significantly lower than those of the DMFCs with 4 M KOH + 2 M methanol fuel (P.D.$_{max}$ = 26.09 mW cm^{-2}) at the same amount of catalyst loadings on the electrodes (that is, the anode with 4 mg cm^{-2} PtRu black ink and the cathode with 4 mg cm^{-2} MnO_2/C ink). The peak power density value of the ADMFC with pure methanol fuel was decreased at an approximate two-order magnitude, as compared with that of the ADMFC with a mixture fuel containing both KOH electrolyte and methanol fuel. It is assumed that the KOH electrolyte played a vital role in improving the performance of alkaline DMFC.

From the point of view of the application, the material cost is a crucial factor. It was demonstrated that the alkaline DMFC consists of the air electrode using a non-precious metal catalyst (that is, a low-cost MnO_2 catalyst instead of an expensive Pt, can be effectively used). It was found that a metal oxide catalyst of MnO_2 is not only inexpensive but also more tolerant towards crossover, and is active for the reduction of O_2 to OH^- in an alkaline media. The as-prepared QPVA/20 wt.%Q-SiO_2/5 wt.%GA composite membrane is a low-cost non-perfluorosulfonated polymer membrane, as compared with an expensive Nafion membrane.

4. Conclusions

The anion-exchange composite membrane based on QPVA and Q-SiO_2 fillers was prepared by a solution casting method. It demonstrates that the ionic conductivity of PVA polymer membranes significantly increases via by an amination process using GTMAC. An alkaline direct methanol fuel cell comprising of the QPVA/Q-SiO_2 composite membrane was assembled and systematically examined. The highest peak power density of alkaline DMFC comprising of QPVA/20 wt.%Q-SiO_2 composite membrane with 4 mg cm^{-2} PtRu black with a 8 M KOH + 2 M CH_3OH fuel is approximately 35.13 mW cm^{-2} at 50 °C. However, the peak power density value of the DMFC with pure 2 M methanol fuel is approximately 0.27 mW cm^{-2}. From the practical point of view, QPVA/Q-SiO_2 composite membrane can be fabricated by a simple blending process. The anion-exchange QPVA/Q-SiO_2 composite membranes are viable candidate for applications in alkaline DMFCs.

Acknowledgement

Financial support from the National Science Council, Taiwan (Project No: NSC-96-2221-E131-009-MY2) is gratefully acknowledged.

References

[1] C.C. Yang, J. Membr. Sci. 288 (2007) 51–60.
[2] C.C. Yang, S.J. Chiu, W.C. Chien, J. Power Sources 162 (2006) 21–29.
[3] Y. Wang, L. Li, L. Hu, L. Zhuang, J. Lu, B. Xu, Electrochem. Commun. 5 (2003) 662–666.
[4] V. Baglio, A.S. Arico, A.D. Blasi, V. Antonucci, P.L. Antonucci, S. Licoccia, E. Traversa, F.S. Fiory, Electrochim. Acta 50 (2005) 1241–1246.
[5] S. Panero, P. Fiorenza, M.A. Navarra, J. Romanowska, B. Scrosati, J. Electrochem. Soc. 152 (12) (2005) A2400–A2405.
[6] H.Y. Chang, C.W. Lin, J. Membr. Sci. 218 (2003) 295–306.
[7] C. Xu, P.K. Shen, X. Ji, R. Zeng, Y. Liu, Electrochem. Commun. 7 (2005) 1305–1308.
[8] K. Matsuoka, Y. Iriyama, T. Abea, M. Matsuoka, Z. Ogumia, J. Power Sources 150 (2005) 27–31.
[9] J.J. Kang, W.Y. Li, Y. Lin, X.P. Li, X.R. Xiao, S.B. Fang, Polym. Adv. Technol. 15 (2004) 61–64.
[10] E.H. Yu, K. Scott, J. Appl. Electrochem. 35 (2005) 91–96.
[11] L. Li, Y.X. Wang, J. Membr. Sci. 262 (2005) 1–4.
[12] J.R. Varcoe, R.C.T. Slade, Fuel Cell 5 (2005) 187–200.
[13] T.N. Danks, R.C.T. Slade, J.R. Varcoe, J. Mater. Chem. 13 (2003) 712–721.
[14] R.C.T. Slade, J.R. Varcoe, Solid State Ionics 176 (2005) 585–597.
[15] J. Fang, P.K. Shen, J. Membr. Sci. 285 (2006) 317–322.
[16] Y. Xiong, J. Fang, Q.H. Zeng, Q.L. Liu, J. Membr. Sci. 311 (2008) 319–325.
[17] Y. Xiong, Q.L. Liu, A.M. Zhu, S.M. Huang, Q.H. Zeng, J. Power Sources 186 (2009) 328–333.
[18] Y. Xiong, Q.L. Liu, Q.G. Zheng, A.M. Zhu, J. Power Sources 183 (2008) 447–453.
[19] A.A. Mohamad, A.K. Arof, Mater. Lett. 61 (2007) 3096–3099.
[20] S. Sang, J. Zhang, Q. Wu, Y. Liao, Electrochim. Acta 52 (2007) 7315–7321.
[21] C.C. Yang, S.J. Chiu, W.C. Chien, S.S. Chiu, J. Power Sources 195 (2010) 2212–2219.
[22] E.D. Wang, T.S. Zhao, W.W. Yang, Int. J. Hydrogen Energy 35 (2010) 2183–2189.
[23] B. Bae, D. Kim, J. Membr. Sci. 220 (2003) 75–87.
[24] J. Kim, B. Kim, B. Jung, J. Membr. Sci. 207 (2002) 129–137.
[25] C.C. Yang, S.T. Hsu, W.C. Chien, M.C. Shih, S.J. Chiu, K.T. Lee, C.L. Wang, Int. J. Hydrogen Energy 31 (2006) 2076–2087.
[26] Y.H. Yu, C.Y. Lin, J.M. Yeh, W.H. Lin, Polymer 44 (2003) 3553–3560.
[27] Z. Peng, L.X. Kong, S.D. Li, Synth. Met. 152 (2005) 25–28.
[28] C.C. Yang, S.Y.J. Li, T.H. Liou, Desalination 276 (2011) 366–372.
[29] A. Santasalo, S. Hietala, T. Rauhala, T. Kallio, J. Power Sources 196 (2011) 6153–6159.